J. Mech. Phys. Solids Vol. 41, No. 6, pp. 1119–1135, 1993.
Printed in Great Britain.

0022–5096/93 $6.00 + 0.00

THE INFLUENCE OF PLASTICITY ON MIXED MODE INTERFACE TOUGHNESS

VIGGO TVERGAARD

Solid Mechanics Department, Technical University of Denmark, Lyngby, Denmark

and

JOHN W. HUTCHINSON

Division of Applied Sciences, Harvard University, Cambridge, MA, U.S.A.

(*Received* 3 *September* 1992; *in revised form* 16 *November* 1992)

ABSTRACT

CALCULATIONS are reported for the mixed mode toughness of an interface joining an elastic–plastic solid to a solid which does not yield plastically. A potential function of the components of the crack face displacements is used to generate the tractions along the interface where the fracture processes causing separation occur. The two main parameters characterizing this potential are the work of separation per unit area and a peak normal stress. This description of the interface separation process is embedded within the continuum description as a boundary condition on the interface linking the adjoining solids. Small-scale yielding in plane strain is considered with the remote field specified by the magnitude and phase of the mixed mode stress intensity factors. Crack growth resistance curves are computed for a range of the most important nondimensional material parameters and for various combinations of remote mixed mode loading. Particular emphasis is placed on the ratio of the steady-state interface toughness to the "intrinsic" work of separation as it depends on plastic yielding and on the combination of modes 1 and 2. Plasticity enhances the interface toughness for all modes of loading, but substantially more so in the presence of a significant mode 2 component of loading than in near-mode 1 conditions.

1. INTRODUCTION

PLASTIC DEFORMATION comprises a major component of the total work of fracture in ductile materials. Recent experimental work on the mixed mode toughness of interfaces has highlighted the importance of this role of plasticity and at the same time has served to re-emphasize how difficult it is to quantify this role theoretically. Measurements of the toughnesses of interfaces between solids where at least one is ductile (e.g. CAO and EVANS, 1989; LIECHTI and CHAI, 1992; THOULESS, 1990; O'DOWD *et al.*, 1992) have revealed an exceptionally strong dependence on the mode of loading, with near-mode 2 toughness in some systems as much as a factor of 10 higher than near-mode 1 toughness (measured in units of energy per unit area). While it is not at all clear that this mode effect is entirely due to plasticity, it does appear likely that plasticity is the main contributor. For brittle interfaces, EVANS and HUTCHINSON (1989) have proposed a model of asperity interaction behind the crack tip to account for a mixed mode dependence of interface toughness. However, as argued by LIECHTI

and CHAI (1992), the asperity model does not appear to account for the strong toughness dependence on mode when one of the solids has appreciable ductility. Theoretical work on the elastic–plastic interface crack problem by a number of workers (SHIH and ASARO, 1988; ZYWICZ and PARKS, 1992; BOSE and PONTE CASTANEDA, 1992; MATAGA and PONTE CASTANEDA, 1992; SHIH, 1991; LIECHTI and CHAI, 1992) has given insight into possible explanations for a strong mixed mode effect due to plasticity. For a given level of loading, as measured for example by the overall energy release rate G in small-scale yielding, the near-mode 1 loadings have the highest levels of normal traction acting across the interface ahead of the tip in the plastic zone. For prescribed levels of G, the near-mode 2 loadings produce plastic zones which are approximately twice as large as those for the near-mode 1 loadings. While results such as these are highly suggestive and inform the mixed mode problem, they don't constitute toughness predictions.

A predictive model must incorporate a local fracture criterion of some kind which characterizes the fracture process on the interface deep within the plastic zone. Ideally, the model would partition the work that goes into plastic dissipation from that which is absorbed by the local fracture processes required to separate the interface. The steps in the development of a model which incorporates a law governing the tractions involved in interface separation have been taken by NEEDLEMAN (1987, 1990). He embedded the local separation law in a continuum elastic–plastic description of the solids joined across an interface, and he carried out interface cracking calculations using finite element procedures for a number of applications, including particle debonding in a plastically deforming solid. Crack initiation and subsequent growth is calculated directly in terms of the parameters characterizing the separation law and the continuum properties of the solids. TVERGAARD (1990) continued the development of this approach with application to debonding and pullout of fibers in an elastic–plastic matrix.

The present paper applies this same general approach to predict mixed mode toughness of an interface joining one solid which is ductile with another which is not. The present work is a continuation of an earlier study by TVERGAARD and HUTCHINSON (1992), which hereafter will be referred to as T&H, in which such "first principles" predictions were made for the mode 1 toughness of a homogeneous elastic–plastic solid. That study, which will be briefly reviewed in the next section, presented results for the enhancement of toughness due to plastic deformation as it depends on the primary parameters of the fracture process and the continuum properties of the solid. The approach is capable of partitioning the total steady-state work of fracture into the work of the fracture processes and the plastic dissipation occurring in the surrounding plastic zone. In the present study a separation law for the interface is introduced which is derived from a potential of the normal and tangential crack face displacements. It generalizes the separation law used in T&H which involved only normal crack face displacements. The work per unit area needed to separate the interface, Γ_0, is independent of the combination of crack face displacements which lead to separation. This separation law is embedded in the continuum description of the two adjoining solids as a boundary condition along the interface line, precisely as in the earlier work of Needleman, Tvergaard and T&H. In the absence of plasticity, the model predicts the mode-independent interface toughness Γ_0. The thrust of this paper is to use the

model to isolate the influence of plasticity on mixed mode crack growth resistance and toughness and to establish the enhancement of toughness above Γ_0. Asperity interaction behind the crack tip, as modeled by EVANS and HUTCHINSON (1989), is not taken into account. If present, it would contribute an additional source of mixed mode toughness.

An approach with a number of common features but applied at a much finer scale was taken by BELTZ and RICE (1991) who used a displacement potential to model separation of an interface between elastic solids under mixed mode loading. They determined the range of mixed mode loadings such that the crack advanced by separation of the crack faces (interpreted as cleavage) and the complementary range in which the nature of the tangential crack face displacements suggests that dislocations will be emitted. SUO *et al.* (1992) have considered a model which falls between the present model and that of Beltz and Rice. They envision a crack tip which does not emit dislocations and propose a model which consists of a dislocation-free crack tip core region shielded by a plastic zone under small-scale yielding conditions. They compute the relation of the near-tip energy release rate to the applied energy release rate and in this way they can partition the work of separation from the work absorbed by plastic dissipation.

1.1. *The traction–separation law of the interface*

The fracture process associated with the traction–separation law introduced below is not specified at this stage. In the mode 1 study of T&H, several processes were considered in some detail, including void nucleation, growth and coalescence, and second-phase particle crack-bridging. It is not expected that the approach as it is introduced here will apply directly to atomic separation processes on the interface without the addition of more refinements. The dominant scale of the fracture process in many interface systems can indeed be measured in microns rather than nanometers. Thus, the traction–separation law for the interface should be regarded as a phenomenological characterization of the zone where the separation takes place along the interface and not a description of atomic separation. In principle, the fracture process parameters introduced below might be identified, or inferred, by carrying out a few well chosen experiments or they might be predicted using a micromechanical model, as was done for the case of the void failure mechanism in T&H.

Let δ_n and δ_t be the normal and tangential components of the crack face displacements across the interface in the zone where the fracture processes are occurring, as indicated in the insert in Fig. 1. Let δ_n^c and δ_t^c be special values of these components,

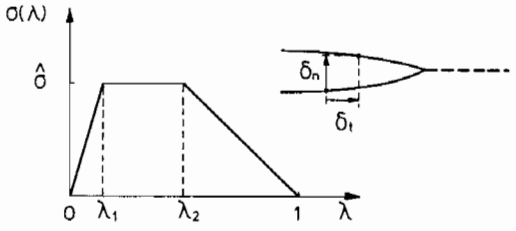

FIG. 1. Traction–generalized displacement relation used to characterize interface separation.

and define a nondimensional crack separation measure as

$$\lambda = \sqrt{(\delta_n/\delta_n^c)^2 + (\delta_t/\delta_t^c)^2} \tag{1.1}$$

such that the tractions drop to zero when $\lambda = 1$. With $\sigma(\lambda)$ displayed in Fig. 1, define a traction potential as

$$\Phi(\delta_n, \delta_t) = \delta_n^c \int_0^\lambda \sigma(\lambda')\, d\lambda'. \tag{1.2}$$

The normal and tangential components of the traction acting on the interface in the fracture process zone are therefore

$$T_n = \frac{\partial \Phi}{\partial \delta_n} = \frac{\sigma(\lambda)}{\lambda} \frac{\delta_n}{\delta_n^c}, \quad T_t = \frac{\partial \Phi}{\partial \delta_t} = \frac{\sigma(\lambda)}{\lambda} \frac{\delta_n^c}{\delta_t^c} \frac{\delta_t}{\delta_t^c}. \tag{1.3}$$

The traction law under a pure normal separation ($\delta_t = 0$) is $T_n = \sigma(\lambda)$ where $\lambda = \delta_n/\delta_n^c$; while under a pure tangential displacement ($\delta_n = 0$), $T_t = (\delta_n^c/\delta_t^c)\sigma(\lambda)$ where $\lambda = \delta_t/\delta_t^c$. The peak normal traction under pure normal separation is $\hat{\sigma}$ and the peak shear traction is $(\delta_n^c/\delta_t^c)\hat{\sigma}$ in a pure tangential displacement. The work of separation per unit area of interface Γ_0 is given by (1.2) with $\lambda = 1$. For the relation $\sigma(\lambda)$ specified in Fig. 1,

$$\Gamma_0 = \tfrac{1}{2}\hat{\sigma}\delta_n^c[1 - \lambda_1 + \lambda_2]. \tag{1.4}$$

The parameters governing the separation law are $\hat{\sigma}$, δ_n^c, δ_t^c together with the shape factors λ_1 and λ_2. Equivalently, the parameters can be taken as Γ_0, $\hat{\sigma}$, δ_n^c/δ_t^c, λ_1 and λ_2.

1.2. *Properties of the two solids*

The solid below the interface is taken to be elastic with Young's modulus E_s and Poisson's ratio ν_s. The elastic properties of the solid above the interface are designated by E and ν. The tensile true stress–true strain behavior for the solid above the interface is specified by

$$\begin{aligned} \varepsilon &= \sigma/E && \text{for} \quad \sigma \leqslant \sigma_Y \\ &= (\sigma_Y/E)(\sigma/\sigma_Y)^{1/N} && \text{for} \quad \sigma > \sigma_Y \end{aligned} \tag{1.5}$$

where σ_Y is the yield stress and N is the strain hardening exponent. The yield surface is taken to be the isotropic hardening surface of Mises.

2. MODE 1 CRACK GROWTH RESISTANCE IN A HOMOGENEOUS MATERIAL

As background for the present study on mixed mode interface fracture, selected results from the earlier mode 1 study of T&H will be presented. The solid is homogeneous and characterized by (1.5). Small-scale yielding in plane strain mode 1 was analysed where the traction law on the crack line in the process zone is the pure normal separation version of (1.3), i.e. $T_n = \sigma(\lambda)$ where $\lambda = \delta_n/\delta_n^c$. Define reference quantities K_0 and R_0 as

$$K_0 = [E\Gamma_0/(1-\nu^2)]^{1/2} \tag{2.1}$$

$$R_0 = \frac{1}{3\pi}\left(\frac{K_0}{\sigma_Y}\right)^2 = \frac{1}{3\pi}\frac{E\Gamma_0}{(1-\nu^2)\sigma_Y^2}. \tag{2.2}$$

Thus, K_0 represents the mode 1 stress intensity factor needed to advance the crack when plastic dissipation is negligible, or, in other words, the stress intensity factor needed to supply just the work of the fracture process Γ_0. The reference length R_0 scales with the size of the plastic zone when $K \cong K_0$; $(K/\sigma_Y)^2/(3\pi)$ is commonly used to estimate the size of the plastic zone in plane strain.

Dimensional considerations dictate that the crack growth resistance $K_R(\Delta a)$, where K_R is the stress intensity factor at crack advance Δa under monotonic conditions, will depend on the various parameters of the solid and the separation law in the following way

$$\frac{K_R(\Delta a)}{K_0} = F\left[\frac{\Delta a}{R_0}, \frac{\hat{\sigma}}{\sigma_Y}, N, \frac{\sigma_Y}{E}, \nu, \lambda_1, \lambda_2\right]. \tag{2.3}$$

The calculation of T&H reveals that, in addition to $\Delta a/R_0$, $\hat{\sigma}/\sigma_Y$ and N were the two most important parameters controlling crack growth resistance with the others in (2.3) playing a secondary role. Figure 2(a) displays crack growth resistance curves for $N = 0.1$ for several levels of $\hat{\sigma}/\sigma_Y$. Steady-state resistance,

$$K_{ss} = \lim_{\Delta a \to \infty} K_R(\Delta a), \tag{2.4}$$

is plotted as a function of $\hat{\sigma}/\sigma_Y$ in Fig. 2(b) for three levels of strain hardening.

In steady state, the ratio of the total work of fracture to the work of the separation process is given by $(K_{ss}/K_0)^2$. From Fig. 2 it is seen that plasticity will only make a significant contribution to the total work of fracture if $\hat{\sigma}/\sigma_Y$ exceeds 2. When $\hat{\sigma}/\sigma_Y$ is less than 2 a fully developed plastic zone cannot develop at the crack tip, as discussed more fully in T&H. Another significant finding which emerged from the earlier work is that the fracture process zone can extend well into the plastic zone. Similar details will be spelled out for the mixed mode problem.

3. Plane Strain Interface Crack in Small-scale Yielding

A schematic drawing of the mixed mode small-scale yielding problem is shown in Fig. 3. The elastic solution governing the remote field of a semi-infinite interface crack is the dominant crack tip singularity field (Rice, 1988). That field has tractions acting on the interface which are given in terms of the two stress intensity factor components, K_1 and K_2, by

$$\sigma_{22} + i\sigma_{12} = (K_1 + iK_2)(2\pi r)^{-1/2} r^{-i\varepsilon} \tag{3.1}$$

where r is the distance from the tip and $i = \sqrt{-1}$. Here ε is the oscillation index

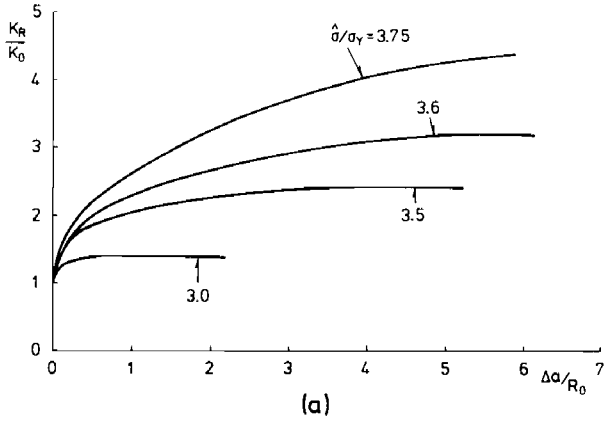

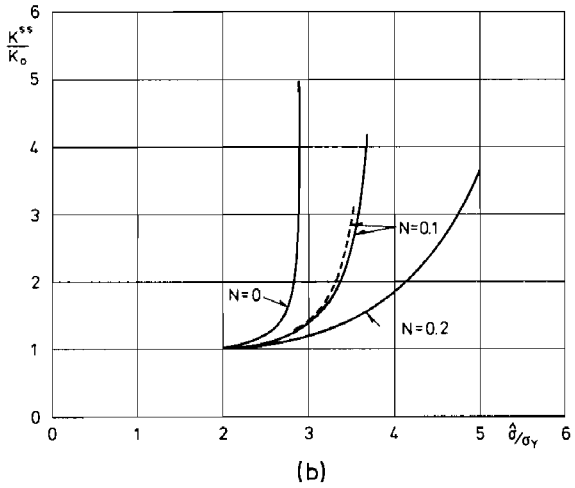

FIG. 2. (a) Mode 1 crack growth resistance curves for a crack advancing in an homogeneous elastic–plastic material with $N = 0.1$, $\nu = 1/3$ and $\sigma_Y/E = 0.003$. (b) Steady-state toughness at three levels of strain hardening. The solid line curves are for $\sigma_Y/E = 0.003$ and the dashed line curve is for $\sigma_Y/E = 0.006$. These curves are from TVERGAARD and HUTCHINSON (1992).

$$\varepsilon = \frac{1}{2\pi} \ln\left(\frac{1-\beta}{1+\beta}\right) \tag{3.2}$$

and β is the second Dundurs' parameter

$$\beta = \frac{1}{2} \frac{\mu(1-2\nu_s) - \mu_s(1-2\nu)}{\mu(1-\nu_s) + \mu_s(1-\nu)} \tag{3.3}$$

with $\mu = E/(2(1+\nu))$ and $\mu_s = E_s/(2(1+\nu_s))$. Let the magnitude of the stress intensity factors be defined by

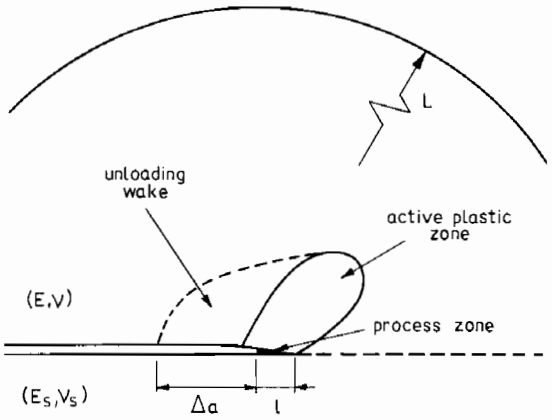

FIG. 3. Schematic of the small-scale yielding interface crack problem.

$$|K| = \sqrt{K_1^2 + K_2^2}. \tag{3.4}$$

The relation between the energy release rate and this magnitude of stress intensity is

$$G = \tfrac{1}{2}(1-\beta^2)\left[\frac{1-\nu^2}{E} + \frac{1-\nu_s^2}{E_s}\right]|K|^2. \tag{3.5}$$

Let L be a reference length characterizing the remote field to be defined in the next section and define an L-dependent measure of mode mixity ψ by

$$\tan\psi = \frac{\operatorname{Im}[(K_1 + iK_2)L^{i\varepsilon}]}{\operatorname{Re}[(K_1 + iK_2)L^{i\varepsilon}]} \tag{3.6}$$

which reduces to the more familiar measure, $\tan\psi = K_2/K_1$, when $\varepsilon = 0$. The interpretation of ψ is aided by using (3.1) in (3.6) giving $\tan\psi = \sigma_{12}/\sigma_{22}$ at $r = L$ on the interface. Thus, ψ measures the relative proportion of shear to normal stress on the interface a distance L from the tip, as predicted by the elastic solution. The displacement components associated with the singularity field in the upper half-space ($\theta > 0$) are given by

$$\mu(u_1 + iu_2) = \frac{|K|r^{1/2}}{2\sqrt{2\pi}\cosh(\pi\varepsilon)}\left\{\frac{(3-4\nu)\,e^{i\theta/2 + \varepsilon(\theta-\pi) - i\bar{\psi}}}{1-2i\varepsilon} - \frac{e^{-i\theta/2 - \varepsilon(\theta-\pi) - i\bar{\psi}}}{1-2i\varepsilon} - i\sin\theta\, e^{i\theta/2 + \varepsilon(\theta-\pi) + i\bar{\psi}}\right\} \tag{3.7}$$

where $\bar{\psi}$ depends on r according to

$$\bar{\psi} = \psi + \varepsilon\ln(r/L). \tag{3.8}$$

The expression for the components in the lower half-space is similar in form.

In specifying the small-scale yielding problem, the displacement components u_1 and u_2 given by (3.7) are imposed remotely on a boundary at $r = R_\infty$, where R_∞ is typically

several times L. The remote loading is thus specified by $|K|$, ψ and L. Using (3.5), define a reference intensity factor to generalize (2.1) according to

$$K_0 = \left[\frac{1-\nu^2}{E} + \frac{1-\nu_s^2}{E_s}\right]^{-1/2}\left(\frac{2\Gamma_0}{1-\beta^2}\right)^{1/2}. \tag{3.9}$$

Thus, K_0 represents the value of $|K|$ needed to advance the interface crack in the absence of any plasticity. As already emphasized, this value is independent of ψ, a deliberate consequence of using a potential to generate the relation of tractions to crack face displacements of the interface. Let R_0 be again defined in terms of K_0 just as in the homogeneous case (2.2), i.e.

$$R_0 = \frac{1}{3\pi}\left(\frac{K_0}{\sigma_Y}\right)^2 = \frac{2}{3\pi}\left[\frac{1-\nu^2}{E} + \frac{1-\nu_s^2}{E_s}\right]^{-1}\frac{\Gamma_0}{(1-\beta^2)\sigma_Y^2}. \tag{3.10}$$

Since R_0 is the length quantity which scales with the size of the plastic zone (when $|K| \cong K_0$) and the fracture process zone length, it is natural to define another measure of mixity, ψ_0, based on the reference length R_0 rather than L in (3.6). By (3.8), ψ and ψ_0 are related by

$$\psi_0 = \psi + \varepsilon \ln (R_0/L). \tag{3.11}$$

For the numerical examples presented below, $\varepsilon = 0.0813$ and R_0/L varies from about 0.002 to 0.004 corresponding to a phase shift $\varepsilon \ln (R_0/L)$ varying between $-25°$ and $-30°$.

4. FINITE ELEMENT MODEL AND CHOICE OF PARAMETERS

The finite strain formulation and numerical finite element scheme used here is the same in almost all respects as that used and described in the earlier study of T&H in Section 2. The reader is referred to that section for details which will not be repeated here. A Mises yield condition is used to generalize the uniaxial relation to multi-axial states. The tractions generated by the separation potential (1.2) are taken as true tractions rather than nominal tractions. This has some influence since there is some readjustment in crack face area due to finite straining in the vicinity of the crack tip, but the effect is not a dominant one.

The number of nondimensional parameters in the mixed mode interface model is large. Crack growth resistance can be written in the nondimensional form (2.3) with the inclusion of the following additional nondimensional parameters: δ_t^c/δ_n^c, δ_n^c/L, ψ, E/E_s and ν_s. In all, the model has 12 nondimensional parameters. Aside from the difficulty of presenting the functional dependencies on such a large parameter set, the calculations themselves are computationally intensive. A single resistance curve such as that presented in Fig. 6 requires up to 75 h of CPU time on a relatively fast work station. For these reasons, we have focused on dependencies on the few most important variables and have relied on the earlier mode 1 study for insight into the role of some of the other parameters. The numerical results presented below have all been computed for the case of a rigid lower half-space ($E_s \to \infty$). This has two benefits. It reduces the

set of parameters by two, and it means that only the upper half-space need be meshed, significantly reducing the size of the numerical problem. As remarked upon later, it is felt that the mixed mode toughness predictions will not be strongly affected by neglecting the elasticity of the lower material as long as the elastic mismatch is properly taken into account in shifting from the near-tip field to the remote loading. The material above the interface has

$$\nu = 1/3, \quad \sigma_Y/E = 0.003, \quad N = 0.1. \tag{4.1}$$

The roles of σ_Y/E and N were studied in T&H [e.g. see Fig. 2(b)] for the mode 1 problem for the homogeneous material. They are expected to play similar roles in the mixed mode problem; they have been fixed at the representative values chosen above. The rigid lower half-space together with $\nu = 1/3$ gives from (3.3) and (3.2)

$$\beta = -1/4 \quad \text{and} \quad \varepsilon = 0.0813. \tag{4.2}$$

The two primary parameters which will be varied in the numerical computations are $\hat{\sigma}/\sigma_Y$ and ψ, one characterizing the separation law and the other the mixed mode loading. In most of the computations the choices

$$\delta_t^c/\delta_n^c = 1, \quad \lambda_1 = 0.15, \quad \lambda_2 = 0.5 \tag{4.3}$$

have been used but a few results will be reported with other values of δ_t^c/δ_n^c. The "shape" parameters of the separation law, λ_1 and λ_2, were shown in the earlier study to be of secondary importance. With Δ as the size of the smallest elements of the mesh along the interface (see Section 2 of T&H for the mesh layout), the choices for δ_n^c and L are

$$\delta_n^c = 0.05\Delta \quad \text{and} \quad L = 2000\Delta \tag{4.4}$$

so that $\delta_t^c/L = 2.5 \times 10^{-5}$. This choice is not limiting since the L-dependence is known through expressions like (3.11). The outer boundary on which the displacements are prescribed is usually chosen to be $R_\infty = 4.5L$. By (1.4), (3.10) and (4.1)–(4.4), the ratio of the two reference lengths is

$$\frac{R_0}{L} = 0.172 \frac{E}{\sigma_Y} \frac{\hat{\sigma}}{\sigma_Y} \frac{\delta_n^c}{L} = 0.00143 \frac{\hat{\sigma}}{\sigma_Y} \tag{4.5}$$

and it is this ratio which leads to the shift between ψ and ψ_0 noted beneath (3.11).

5. Mixed Mode Predictions

A few results for the plastic zones and interface traction distributions for the stationary crack will be reported first. These have been computed using $\hat{\sigma}/\sigma_Y = 20$, effectively suppressing any separation along the line of the crack (i.e. δ_n^c and R_0 are no longer relevant parameters in these results). More extensive results for the stationary problem can be found in Shih and Asaro (1988), Zywicz and Parks (1992) and

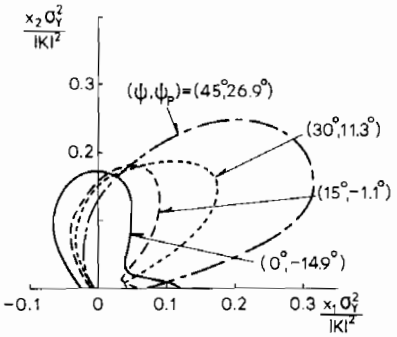

FIG. 4. Small-scale yielding boundaries of the plastic zone of the stationary crack for several mixed mode loadings.

SHIH (1991). Boundaries of the plastic zones are shown in Fig. 4 for four values of ψ. The axes in this figure are the usual ones for small-scale yielding, i.e. $x_i\sigma_Y^2/|K|^2$. For the interface crack problem with nonzero ε one must also specify the ratio of some measure of the plastic zone size to L for the problem to be fully prescribed (since R_0 has been rendered irrelevant). Here the choice R_p/L has been used where

$$R_p = \frac{1}{3\pi}\left(\frac{|K|}{\sigma_Y}\right)^2 \tag{5.1}$$

and an associated phase measure is defined as

$$\psi_p = \psi + \varepsilon \ln (R_p/L). \tag{5.2}$$

For the results presented in Figs 4 and 5 the values of R_p/L taken in the calculations were 0.0409, 0.0314, 0.0180 and 0.0206 for ψ equal to 0°, 15°, 30° and 45°, respectively. The values of both ψ and ψ_p are recorded in the figures.

The normal and shear tractions acting on the interface ahead of the stationary crack discussed above are shown in Fig. 5. The highest normal stress a given distance ahead of the tip is seen to be achieved for the loading with $\psi_p \cong 0°$. This loading might be described as being locally mode 1-like. Given the relatively large shift of phase of about 15° between the local (ψ_p) and remote (ψ) measures of mode mixity, it is clear that the local measure is the most meaningful from the standpoint of thinking about the effect of loading in the vicinity of the plastic zone.

A selection of computed crack growth resistance curves are shown in Fig. 6 plotted as $|K|_R/K_0$ as a function of $\Delta a/R_0$. While an intensity-based presentation has been chosen to present the results, it should be noted that they can be converted immediately to a presentation using the energy release rate. In particular, with Γ_R as the energy release rate needed to advance the crack, by virtue of (3.5) and (3.9)

$$\Gamma_R/\Gamma_0 = (|K|_R/K_0)^2. \tag{5.3}$$

Crack growth initiates at K_0, or equivalently when $\Gamma_R = \Gamma_0$. This can be understood in terms of the (near) path independence of the J-integral prior to any crack growth using an argument identical to that given in Section 3.1 of T&H. Steady-state condi-

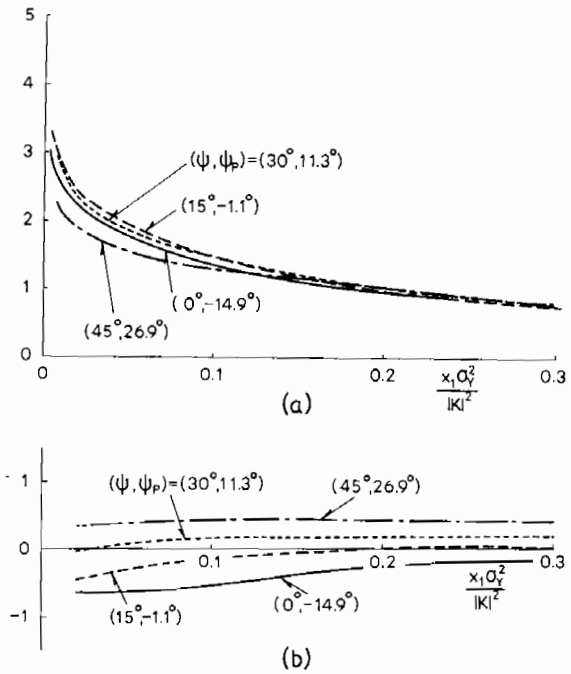

FIG. 5. (a) Normal and (b) tangential tractions on the interface ahead of the stationary crack. In computing these results the parameter $\hat{\sigma}/\sigma_Y$ was taken to be 20 thereby eliminating any influence of the fracture process on these distributions.

tions are attained, to a good approximation, with no further increase in crack growth resistance after advances ranging from a fraction of R_0 to more than five times R_0, depending on $\hat{\sigma}/\sigma_y$ and to a lesser extent on ψ. In almost all instances the steady-state toughness, $|K|_{ss}$, is approached monotonically from below, but there are a few cases such as one shown in Fig. 6 where $|K|_R$ overshoots slightly and then decreases

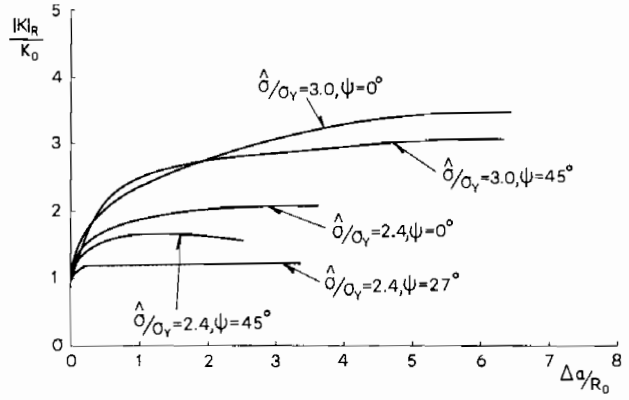

FIG. 6. Interface crack growth resistance curves for various choices of $\hat{\sigma}/\sigma_Y$ and ψ.

somewhat. At the maximum there is a significant tangential contribution to the separation while later on this contribution tends towards zero. The values identified by $|K|_{ss}$ in Fig. 7 below are the peak values of resistance computed and not strictly the steady-state limits, but in all instances the distinction is small. Similar non-monotonic behavior has been predicted for crack growth resistance in transformation toughening materials (STUMP and BUDIANSKY, 1989).

Steady-state mixed mode toughness is plotted as a function of $\hat{\sigma}/\sigma_Y$ in Fig. 7 for several different modes of loading as specified by fixed values of ψ. The values of ψ_0 in (3.11) associated with these curves vary weakly with $\hat{\sigma}/\sigma_Y$ by (4.5), but are less than ψ by between 25° and 30°. Thus, for example, the curve for $\psi = 38°$ has a ψ_0 a little above 0° and is the closest to a mode I loading of those shown. For the curves labeled $\psi = 0°$, 38° and 45°, the separation process is dominated by the normal component of displacement δ_n. The parameter δ_n^c/δ_t^c plays a relatively unimportant role in these cases. On the other hand, for the two curves with $\psi = -45°$ and $-52°$, the tangential component δ_t is much larger than δ_n in the range of low $\hat{\sigma}/\sigma_Y$ and then gradually decreases and becomes comparable to δ_n as $\hat{\sigma}/\sigma_Y$ increases. In these cases the manner in which the tangential interface displacement is included in the separation law has a significant influence on the toughness predictions.

In Fig. 8, the steady-state toughness is plotted as a function of ψ_0 for fixed values of $\hat{\sigma}/\sigma_Y$, in Fig. 8(a) with the choice $\delta_n^c/\delta_t^c = 1$ and in Fig. 8(b) with $\delta_n^c/\delta_t^c = 100$. Recall that the peak stress in a purely tangential displacement of the crack faces is δ_n^c/δ_t^c times the peak stress $\hat{\sigma}$ in a purely normal separation. Thus, the curves in Fig. 8(b) with $\delta_n^c/\delta_t^c = 100$ correspond to an interface law which, for all practical purposes, suppresses any tangential displacement at the interface so that separation must occur by purely normal displacements. While there is some dependence on the parameter δ_n^c/δ_t^c in the separation potential, as will be remarked upon further below, the main influence seen in Fig. 8 is the dependence on $\hat{\sigma}/\sigma_Y$ and ψ_0.

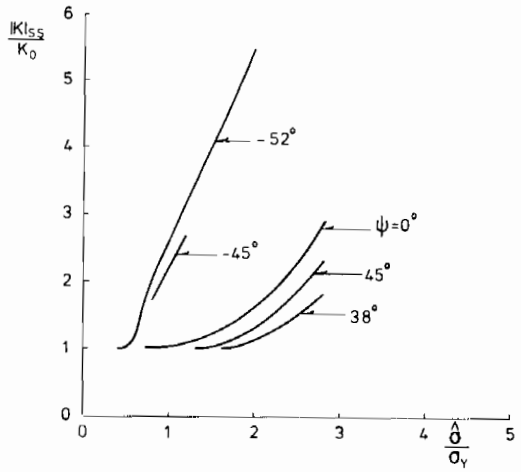

FIG. 7. Steady-state interface toughness for various values of mixed mode loading as specified by the remote mixity measure ψ.

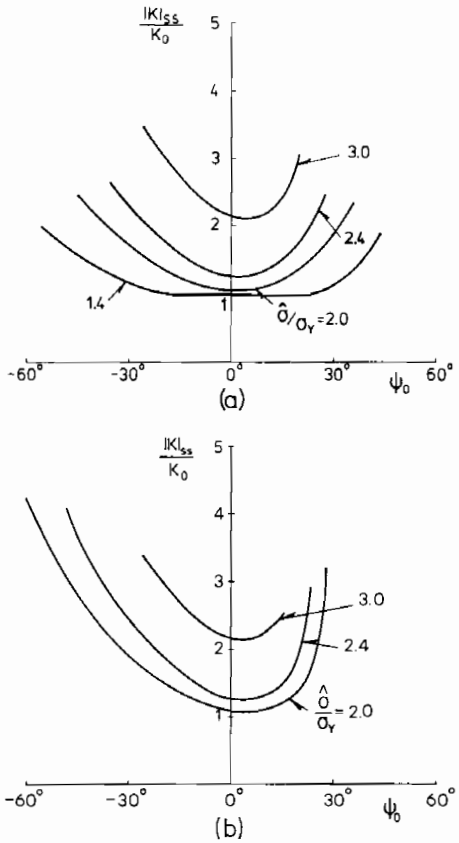

FIG. 8. Steady-state interface toughness as a function of the local mixity measure ψ_0: (a) with $\delta_n^c/\delta_t^c = 1$ and (b) with $\delta_n^c/\delta_t^c = 100$. The case shown in (b) effectively suppresses any relative tangential displacement of the interface in the fracture process zone.

With the exception of the curve in Fig. 8 for $\hat{\sigma}/\sigma_Y = 1.4$ for which plasticity plays a relatively small role, there is a strong mixed mode effect on toughness. The minima of these curves do fall near $\psi_0 = 0$ indicating the merits of using the "local" measure ψ_0 to present the predictions. The strong dependence of the interface toughness on ψ_0 predicted is in agreement with trends observed experimentally in systems where plastic deformation occurs at the crack tip in at least one of the materials joined across the interface (LIECHTI and CHAI, 1992; CAO and EVANS, 1989; THOULESS, 1990; O'DOWD *et al.*, 1992). All the experimental data taken to date for such systems seem to display an increase in toughness accompanying an increase in relative proportion of mode 2 to mode 1. The strong trends seen in Fig. 8 must be attributed to the effect of plasticity since the work of separation Γ_0 is mode-independent and the other details of the separation potential (1.2) seem to be relatively less important, as will be discussed subsequently.

There is some distinct asymmetry in the toughness variations with ψ_0 with respect

to the minima of these curves. The general shape of these curves, including the asymmetry, is roughly consistent with the experimentally measured mixed mode toughness curves obtained by LIECHTI and CHAI (1992) for an epoxy–glass interface. These researchers made careful estimates of the plastic zone sizes under the full range of loadings and verified that the tests were well within the small-scale yielding range for their specimens. There is another feature of the predictions in Fig. 8 which appears to be consistent with data taken for a Niobium–Al_2O_3 interface by O'DOWD *et al.* (1992). These workers could only obtain interface toughness data for $\psi_0 \leqslant 0^\circ$ since the interface crack kinks into the brittle Al_2O_3 for $\psi_0 > 0^\circ$. (Note that these workers take the ductile material to be below the interface so that their phase measure has the opposite sign to that being used here.) However, the toughness data for this interface intersects the vertical axis at $\psi_0 = 0$ with a nonzero slope, much like the curve for $\hat{\sigma}/\sigma_Y = 3$ does. Moreover, the general trend is similar over the range of the present predictions.

The minimum steady-state mixed mode toughness for the interface crack is substantially higher than the mode I steady-state toughness for the homogeneous material at a given value of $\hat{\sigma}/\sigma_Y$. Recall that the solid line curve for $N = 0.1$ in Fig. 2(b) for the mode I toughness was computed with precisely the same material and separation potential parameters as for the mixed mode results in Fig. 8. Thus, for example, the minimum value of $|K|_{ss}/K_0$ for the interface crack with $\hat{\sigma}/\sigma_Y = 3$ is 2.1 while the corresponding value for the mode I crack is only 1.4. Presumably, the constraint of the material below the interface which undergoes no plastic deformation is the source of the relative toughness enhancement. We believe that the curves of mixed mode toughness in Fig. 8, which are plotted in terms of the local measure of mixity, would not be significantly different if they had been calculated using finite values of E/E_s, and even with $E/E_s = 1$, although this assertion has not been verified.

With l_{ss} denoting the length of the process zone, extending from the points along the interface where the peak stress is first attained to the point where $\lambda = 1$, the ratio l_{ss}/R_0 accompanying the results in Fig. 8(a) is shown in Fig. 9. In accordance with the

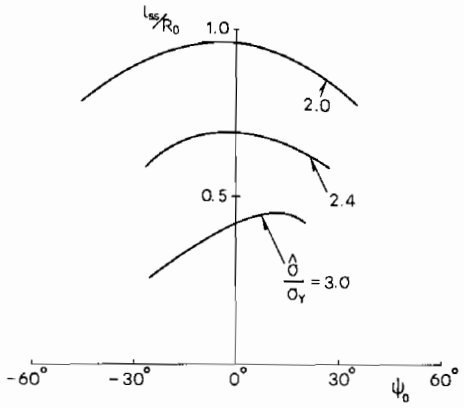

FIG. 9. Normalized length of the steady-state fracture process zone for the case $\delta_n^c/\delta_t^c = 1$.

trends observed for the mode 1 problem, the length of the fracture process zone can be a significant fraction of the plastic zone size when plasticity effects are rather small and diminishes relative to the plastic zone size with increasing $\hat{\sigma}/\sigma_Y$. (Recall that the plastic zone size is approximately equal to R_0 when $\hat{\sigma}/\sigma_Y$ is less than about 2 and becomes large compared to R_0 as $\hat{\sigma}/\sigma_Y$ increases above 2.)

The effect of varying the parameter δ_n^c/δ_t^c is seen in Fig. 10 where the mixed mode toughness prediction is displayed for $\hat{\sigma}/\sigma_Y = 2.4$. As already mentioned, the curve for $\delta_n^c/\delta_t^c = 100$ corresponds to an interface separation law which effectively suppresses tangential interface displacements. The law associated with the curve for $\delta_n^c/\delta_t^c = 0.5$ has a peak stress in a pure tangential "separation" displacement which is $\hat{\sigma}/2$ making it relatively easier for the interface to separate under loadings with a substantial mode 2 content, as can be seen in the figure. The main conclusion to be drawn from Fig. 10 is that for relatively small amounts of mode 2 (i.e. $|\psi_0| < 20°$) the dependence of the toughness on the tangential component of the displacement of the separation potential as specified by δ_n^c/δ_t^c is of relatively minor consequence but, not surprisingly, becomes more important as the mode 2 content of the loading becomes larger.

6. Discussion and Suggestions for Further Work

The strong dependence of interface toughness on the relative proportion of mode 2 to mode 1 seen in experimental data is predicted by an elastic–plastic continuum model with an embedded traction–displacement law characterizing the fracture process on the interface. The increase in toughness with increasing proportion of mode 2 to mode 1 is predicted to be a consequence of plastic deformation outside of the fracture process zone; the work of the fracture process is modeled as being mode-independent. Studies such as the present one, as well as earlier studies cited, give convincing evidence that "first principles" computation of crack propagation are feasible with present day computational facilities. Approaches which build in the

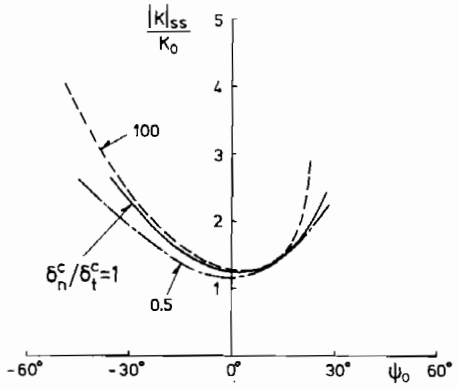

Fig. 10. Influence of the separation law parameter δ_n^c/δ_t^c on the steady-state interface toughness for the case $\hat{\sigma}/\sigma_Y = 2.4$.

fracture process hold promise for linking predictions for small-scale yielding (which can be encompassed by linear elastic fracture methodology) with those for large-scale yielding (for which no universal methodology exists), since no restriction on the extent of the plastic deformation need be imposed.

Computational models which embed a fracture process zone hold promise to circumvent a related difficulty in nonlinear fracture analysis which appears to be particularly acute for interface cracks. Several studies (SHARMA and ARAVAS, 1992; MATAGA and PONTE CASTANEDA, 1992) have shown that the elastic–plastic singularity field of a crack on an interface lying between solids with dissimilar elastic–plastic properties usually has an exceedingly small domain of dominance. So small, in many instances, that the singular fields have no physical meaning. This state of affairs invalidates any fracture approach based on the near-tip singularity field. An approach based on an embedded model of the fracture process zone does not make use of any notions involving a crack tip singularity field within the plastic zone. Indeed, it was seen that the size of the fracture process zone can be a significant fraction of the size of the plastic zone, a clear indication that a singularity-based approach under such circumstances is doomed. This pessimistic assessment may not always be warranted however. The work of BOSE and CASTANEDA (1992) indicates that under some conditions of interface crack growth the zone of dominance may be large enough to invoke a singularity-based approach. Moreover, these authors discovered that a mode 1-like singular field prevails even when the remote loading as measured by ψ has a significant mode 2 component. These two features lead these authors to propose a growth criterion based on a critical value of the near-tip plastic stress intensity factor, although no predictions are actually made.

While an approach using an embedded fracture process model circumvents the issue of domain of validity of a singularity field, it introduces other problems. In particular, in the present approach, the traction–displacement law must be a sufficiently realistic representation of the actual fracture process such that the parameters Γ_0, σ, δ_n^c, etc. can be inferred from selected experiments or can be computed using micromechanical models. In T&H some initial attempts were made to compute the fracture process parameters for the mechanism of void nucleation, growth and coalescence using a micromechanics model. In the present study of the mixed mode loadings it has been seen that the predictions do not seem to be unusually sensitive to features of the traction–separation law such as the relative peak in the traction stress in pure shear to that in pure normal separation as specified by the parameter δ_n^c/δ_t^c. We have carried out a preliminary study extending that in T&H to include both tangential and normal crack face displacements in the micromechanics model of separation by void growth and coalescence. We find that over a fairly broad range of tangential to normal displacements the work of separation Γ_0 is essentially constant and the value of δ_n^c/δ_t^c is approximately 0.2. This suggests that the toughness curve for such an interface would be somewhat lower than the lowest curve in Fig. 7. The present approach is not tied to the necessity of using a potential to generate the interface tractions, and some calculations have been carried out for potential-less laws. More effort will be necessary to establish the traction–separation laws for specific fracture processes if approaches of the type used here are to be employed as predictive tools.

Acknowledgements

The work of JWH was supported in part by the National Science Foundation under Grants NSF-MSS-90-20141 and NSF-DMR-89-20490 and by the Division of Applied Sciences, Harvard University.

References

Beltz, G. E. and Rice, J. R. (1991) In *Modeling the Deformation of Crystalline Solids* (eds T. C. Lowe *et al.*) The Minerals, Metals and Materials Soc. p. 457. TMS, Warrendale, PA.
Bose, K. and Ponte Castaneda, P. (1992) *J. Mech. Phys. Solids* **40,** 1053.
Cao, H. C. and Evans, A. G. (1989) *Mech. Mater.* **7,** 295.
Evans, A. G. and Hutchinson, J. W. (1989) *Acta Metall.* **37,** 909.
Liechti, K. M. and Chai, Y. S. (1992) *J. Appl. Mech.* **59,** 295.
Mataga, P. A. and Ponte Castaneda, P. (1992) Stable crack growth along a brittle/ductile interface—II. Small scale yielding solutions, to be published.
Needleman, A. (1987) *J. Appl. Mech.* **54,** 525.
Needleman, A. (1990) *J. Mech. Phys. Solids* **38,** 289.
O'Dowd, N. P., Stout, M. G. and Shih, C. F. (1992) Fracture toughness of alumina/niobium interfaces: experiments and analyses. *Phil. Mag.* **A66,** 1037.
Rice, J. R. (1988) *J. Appl. Mech.* **55,** 98.
Sharma, S. M. and Aravas, N. (1993) On the development of variable-separable asymptotic elastoplastic solutions for interface cracks. *Int. J. Solids Struct.* **30,** 695.
Shih, C. F. (1991) *Mater. Sci. Engng* **A143,** 77.
Shih, C. F. and Asaro, R. J. (1988) *J. Appl. Mech.* **55,** 299.
Stump, D. M. and Budiansky, B. (1989) *Int. J. Solids Struct.* **25,** 635.
Suo, Z., Shih, C. F. and Varias, A. G. (1993) A theory for cleavage cracking in the presence of plastic flow. *Acta Met. Mater.*, in press.
Thouless, M. D. (1990) *Acta Met. Mater.* **38,** 1135.
Tvergaard, V. (1990) *Mater. Sci. Engng* **A125,** 203.
Tvergaard, V. and Hutchinson, J. W. (1992) *J. Mech. Phys. Solids* **40,** 1377.
Zywicz, E. and Parks, D. M. (1992) *J. Mech. Phys. Solids* **40,** 511.